Supplementary Materials:

Fig. S1

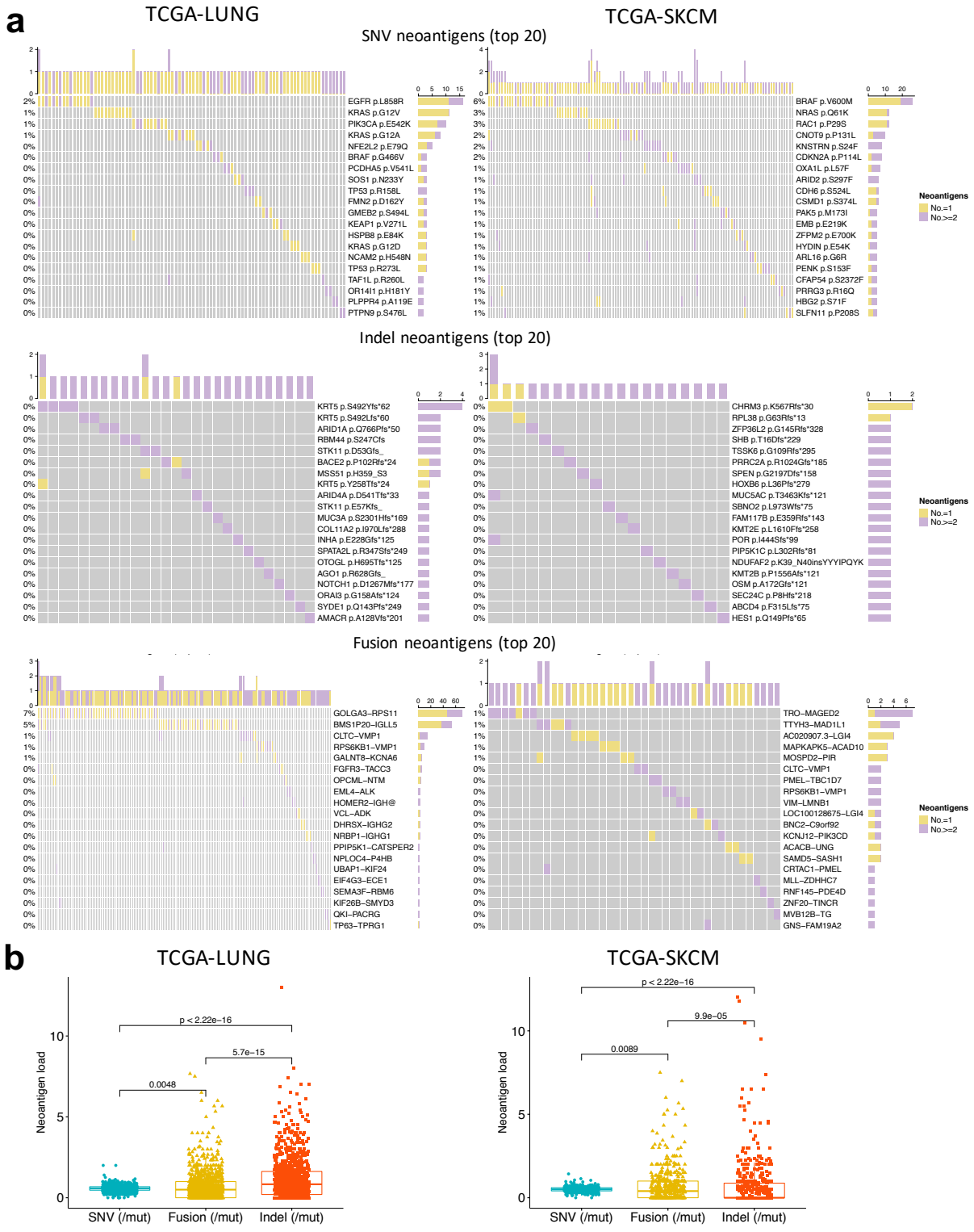

Supplementary Fig. 1. a, The landscape of neoantigens derived from SNVs (top), indels (middle) and fusion genes (bottom) in TCGA-LUNG (left) and TCGA-SKCM (right). **b,** More neoantigens are observed per indel than a SNV or a fusion gene in TCGA-LUNG (left panel); in contrast, neoantigens derived from each of SNVs were found to be more than those from each of fusions and indels in TCGA-SKCM (right panel).

Fig. S2

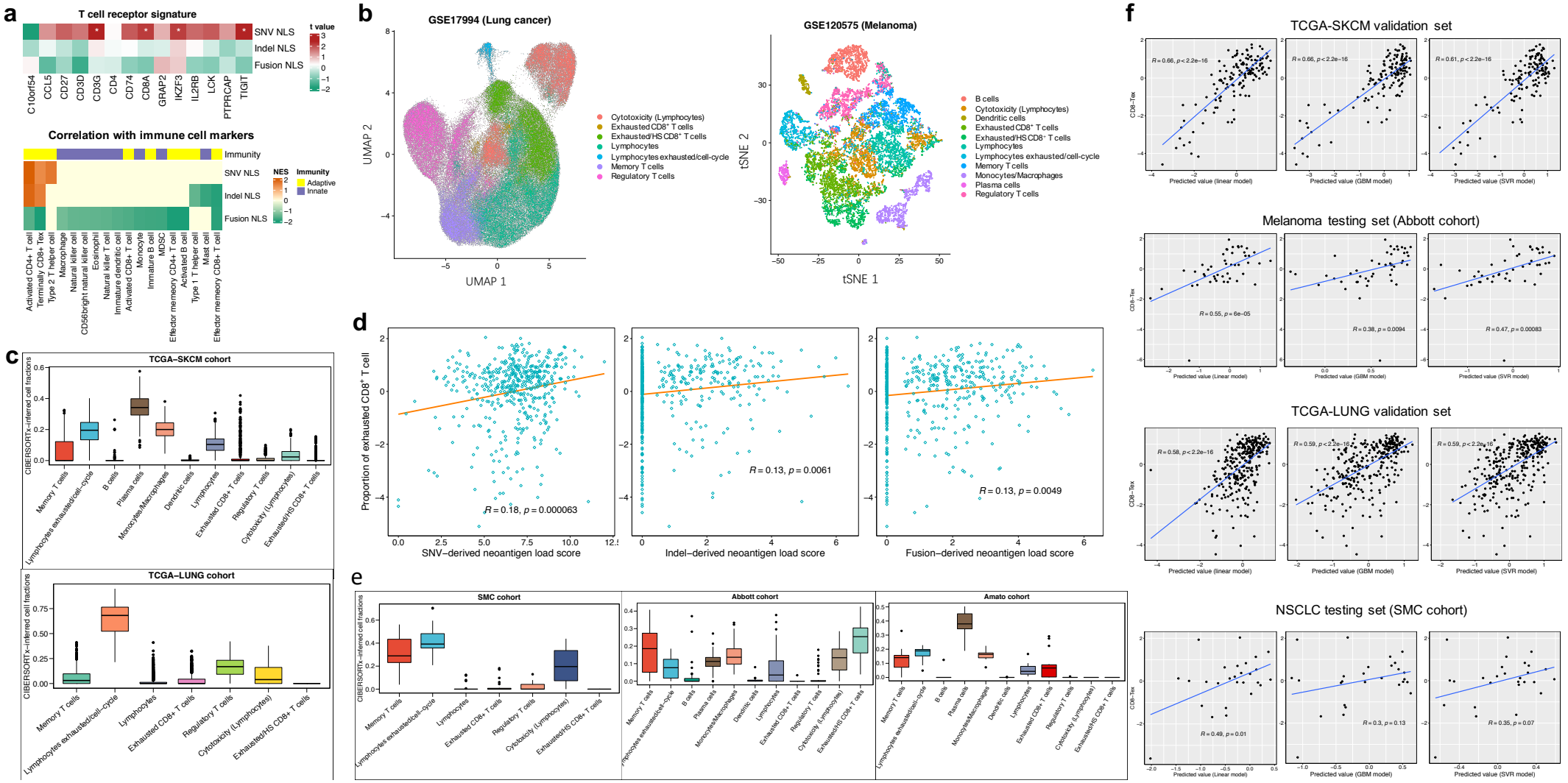

Supplementary Fig. 2. a, Heatmaps of correlations between mRNA expression levels of TCR gene signatures with NLS of three types (top panel), and GSEA normalized enrichment scores (NESs) for immune cell marker genes (bottom panel) in TCGA-SKCM primary samples. **b,** UMAP and tSNE plots of lymphoid and myeloid cells in scRNA-seq datasets of lung cancer and melanoma, colored by broad cell type. **c,** The cell-type fractions inferred using CIBERSORTx in bulk RNA-seq of TCGA-LUNG and TCGA-SKCM samples. **d,** The correlations of SNV-, indel- and fusion-derived NLS with CIBERSORTx-inferred exhausted CD8⁺ T cells in TCGA-SKCM samples. **e,** The cell-type fractions in bulk RNA-seq of ICB samples inferred by CIBERSORTx. **f,** The performance comparison of three models in validation and testing datasets.

Fig. S3

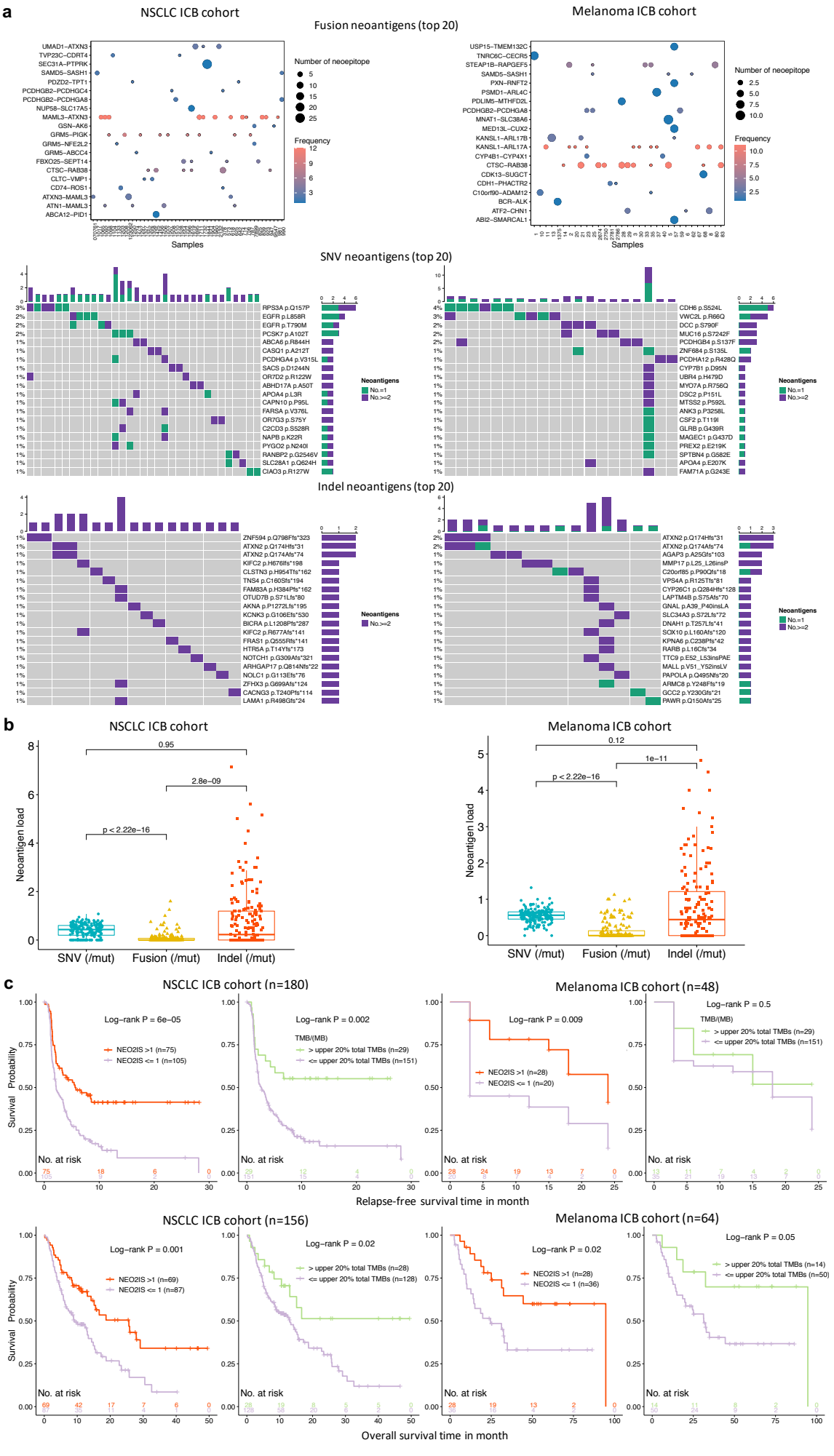
a
NSCLC ICB cohort
Melanoma ICB cohort
Fusion neoantigens (top 20)
Number of neoepitope
Frequency
Samples
SNV neoantigens (top 20)
Indel neoantigens (top 20)
Neoantigens
No.=1
No.>=2
b
NSCLC ICB cohort
Melanoma ICB cohort
Neoantigen load
SNV (/mut)
Fusion (/mut)
Indel (/mut)
p < 2.22e−16
0.95
2.8e−09
0.12
1e−11
c
NSCLC ICB cohort (n=180)
Melanoma ICB cohort (n=48)
Log−rank P = 6e−05
NEO2IS >1 (n=75)
NEO2IS <= 1 (n=105)
Log−rank P = 0.002
TMB/(MB)
> upper 20% total TMBs (n=29)
<= upper 20% total TMBs (n=151)
Log−rank P = 0.009
NEO2IS >1 (n=28)
NEO2IS <= 1 (n=20)
Log−rank P = 0.5
Survival Probability
No. at risk
Relapse-free survival time in month
NSCLC ICB cohort (n=156)
Melanoma ICB cohort (n=64)
Log−rank P = 0.001
NEO2IS >1 (n=69)
NEO2IS <= 1 (n=87)
Log−rank P = 0.02
> upper 20% total TMBs (n=28)
<= upper 20% total TMBs (n=128)
NEO2IS >1 (n=28)
NEO2IS <= 1 (n=36)
Log−rank P = 0.05
> upper 20% total TMBs (n=14)
<= upper 20% total TMBs (n=50)
Overall survival time in month

Supplementary Fig. 3. Neoantigens inferred from ICB cohorts and clinical efficacy evaluated by the NEO2IS and TMB, Related Fig. 3.
a, Neoantigen landscape of combined NSCLC and melanoma ICB cohort and comparison of neoantigen frequency. **b,** The number of candidate neoantigens originating from each SNV or an indel observed to be significantly higher than those from a fusion gene in NSCLC and melanoma external datasets. **c,** Upper panel, Kaplan-Meier (KM) curves for relapse-free survivals according to NEO2IS (left) and TMB (right) in NSCLC and melanoma ICB cohorts; bottom panel, KM curves for overall survivals stratified by NEO2IS (left) and TMB (right) in two ICB cohorts (n=156). NEO2IS>1 and TMB > upper 20% of cohort TMB used as cut-off points.

Fig. S4

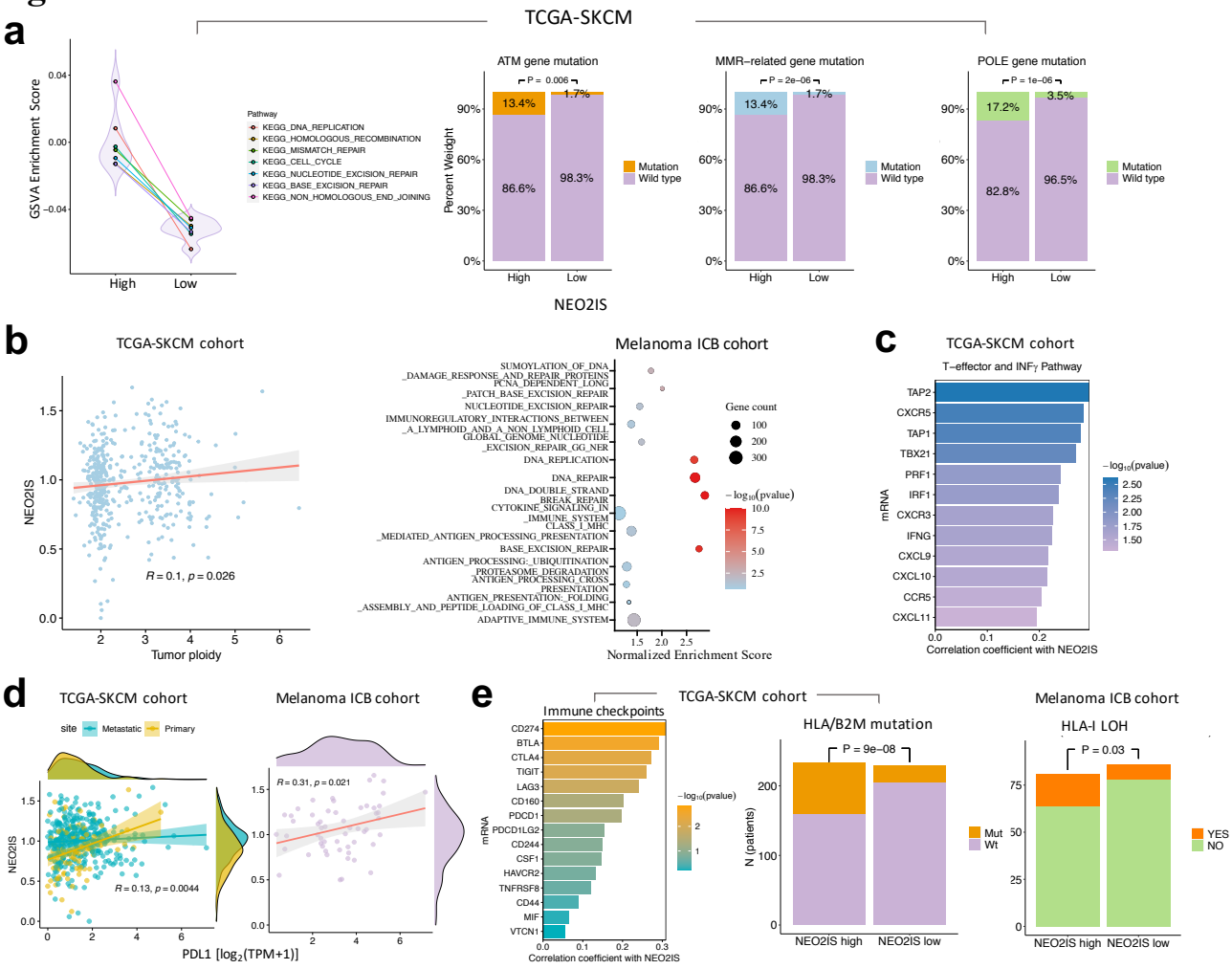

Supplementary Fig. 4. Genomic and molecular features associated with NEO2IS.
a, Left panel, GSVA showing DDR pathways significantly enriched in high NEO2IS group (adjusted p-value < 0.05); right panel, the estimated proportion of ATM, POLE and MMR-related gene mutations in two subgroups divided by median NEO2IS. **b,** Left panel, tumor ploidy significantly related to the neoantigen signature; right panel, GSEA enrichment results (q-value <0.3) for immunomodulatory REACTOME pathways (top 10) that correlated with NEO2IS in external melanoma samples. **c,** Comparison of the mRNA expressions of genes associated with T-effector and INFγ pathway between high and low NEO2IS groups. **d,** NEO2IS shows significant association with PDL1 expression levels (left panel); higher levels of co-inhibitory receptors, LOHHLA and HLA/B2M gene mutations associated with higher NEO2IS (right panel) in melanomas.

Fig. S5

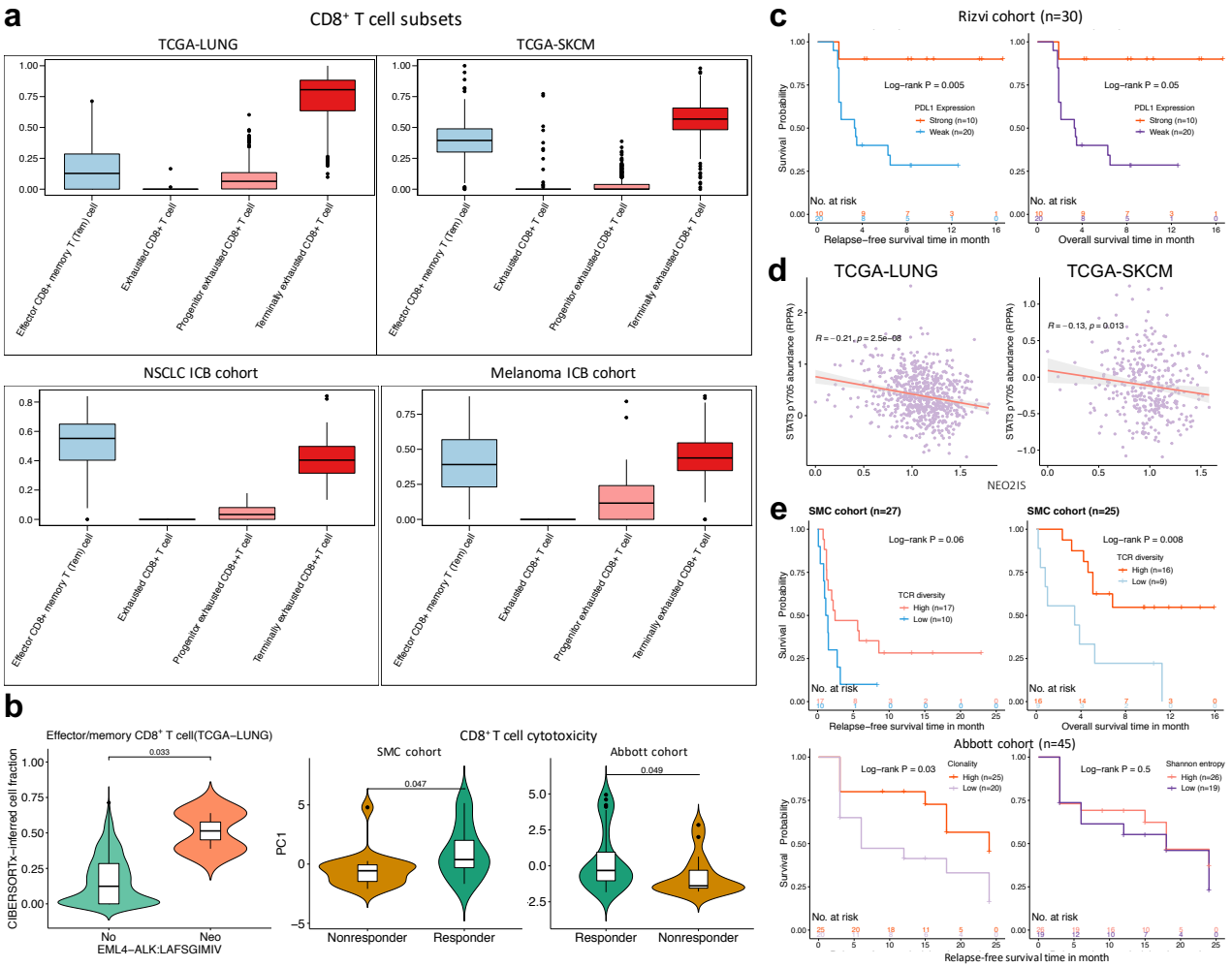

Supplementary Fig. 5. a, CIBERSORTx-estimated cell fractions of CD8⁺ T-cell subsets in bulk RNA-seq datasets. **b,** EML4-ALK-derived LAFSGIMIV with high neoantigen score manifests potential immunogenicity in TCGA-LUNG (left); stronger cytolytic activity observed in responders than nonresponders in NSCLC and melanoma cohorts (middle and right). **c,** Tumors with higher PDL1 expressions exhibit durable clinical response to anti-PD1 treatment (left) and longer overall survival (right) in Rizvi cohort. **d,** NEO2IS correlated significantly with STAT3 pY705 abundance in TCGA tumors. **e,** Kaplan–Meier plots for RFS and OS from SMC and Abbott cohorts stratified by TCR Shannon entropy (upper) and TCR clonality (bottom).